

## ORIGINAL ARTICLE

**Computed Tomography and Cross-Sectional Anatomy of the Metatarsus and Digits of the One-humped Camel (*Camelus dromedarius*) and Buffalo (*Bos bubalis*)**

A. El-Shafey and A. Kassab\*

Address of authors: Department of Anatomy and Embryology, Faculty of Veterinary Medicine (Moshtohor), Benha University, Benha, Egypt

**\*Correspondence:**

Tel.: +20132461411;  
fax: +20132460640;  
e-mail: kassab\_aa@yahoo.com

With 10 figures

Received December 2011; accepted for  
publication June 2012

doi: 10.1111/j.1439-0264.2012.01174.x

**Summary**

The purpose of the present study was to provide a detailed computed tomography (CT) and cross-sectional anatomic reference of the normal metatarsus and digits for the camel and buffalo, as well as to compare between metatarsus and digits in these animals to outstand a basis for diagnosis of their diseases. Advantages, including depiction of detailed cross-sectional anatomy, improved contrast resolution and computer reformatting, make it a potentially valuable diagnostic technique. The hind limbs of 12 healthy adult camel and buffalo were used. Clinically relevant anatomic structures were identified and labelled at each level in the corresponding images (CT and anatomic slices). CT images were used to identify the bony and soft tissue structures of the metatarsus and digits. The knowledge of normal anatomy of the camel and buffalo metatarsus and digits would serve as initial reference to the evaluation of CT images in these species.

**Introduction**

Diseases of the metatarsus and digits in the ruminants are not rare, especially in the buffalo, which necessitates awareness of its normal structure to be able to recognize changes in the diseased animal. Economic importance of the bovine lameness is completely understood, and many research have been carried out in this field for better understanding of the pathogenesis of the bovine hoof and digit problems (Shearer and Van Amstel, 2001).

The bovine digits are a complex structure with joints, ligaments and tendons (Raji et al., 2008). Classical anatomic atlases cannot provide the spectrum of views and the details required in modern diagnostic and surgical techniques (Gehrmann et al., 2006).

Current diagnostic imaging technique such as radiography and ultrasonography provides limited information for evaluation of the bovine digits and hoof. Radiography has limited value to evaluation of soft tissue, although ultrasonography provides visualization of the tendons and ligaments (Kaser-Hotz et al., 1994). However, ultrasonography provides a small field of view and each structure has to be imaged separately, and a cross-sectional examination through the entire digit is not possible. On the

other hand, soft tissue is difficult to be evaluated by ultrasonography in the digits (Denoix et al., 1993).

Computed tomography (CT) was not initially used in veterinary medicine because of its limited accessibility and high costs. However, accessibility has improved, which has increased the need of the use of this technique in cattle (Raji et al., 2008), dogs (Ottesen and Moe, 1998) and horses (Whitton et al., 1998; Tomlinson et al., 2003).

So, the aim of this study was first to describe the normal anatomy metatarsal and digit regions in the images and normal variations in camels and buffaloes with no history of metatarsal or digit region pain. Second, to provide an atlas of detailed CT and cross-sectional anatomy of the metatarsus and digits for the camel and buffalo metatarsus and digits.

**Materials and Methods****Animals**

The present work was carried out on the metatarsus and digits of 12 healthy adult camel and buffalo (six camel of 10–15 years old and six buffalo of 5–7 years old), four males and two females of each species. The selected

animals were subjected to clinical examination before slaughtering for lameness included palpation of the metatarsal bones and joints and a moving examination. The hind limbs were obtained immediately after slaughter, by disarticulating the tarsometatarsal joints, cooled and imaged within 12 h to minimize post-mortem changes.

### CT examination

The limbs were underwent consecutive CT scan using CT scanner [TOSHIBA 600 HQ (third-generation equip TCT), Japan]. A CT scan was carried out in the Radiology Center (Medical Radiology Center, Benha University, Egypt), and contiguous transverse images were obtained. The acquisition settings were 120 kv, 130 mA and 1.5 s, thickness of 3 mm, pitch of 0.625, field of view of 45 cm and matrix size of  $512 \times 512$  pixels. The images were started at the level of the base of the large metatarsal bone, 3 cm distal to the carpal articulation and continuing distally into 1 cm below the distal inter-phalangeal (coffin) joint.

After the CT images were obtained, the limbs were frozen at  $-20^{\circ}\text{C}$  and then sectioned transversely using an electric band saw, to correspond with the CT images. All sections were cleaned, photographed and kept for the future studies.

### Comparison of CT and anatomic images

Important anatomic structures were identified and labelled in two corresponding CT scans and cross-sections of the camel and buffalo metatarsus and digits with the

aid of multiple references (Getty, 1975; Smuts and Bezuidenhout, 1987; Schaller, 1992; Nickel et al., 1996), together with *Nomina Anatomica Veterinaria* (2005). Ten transverse slices from both CT and gross sections were chosen for publication.

Some structures present in the anatomical sections could not be seen on the corresponding CT images and vice versa.

### Results

The results of the study consisted of ten CT images and ten gross cross-sections of the camel and buffalo metatarsus and digits (Figs 1–10). The CT provided good discrimination between bone and soft tissue and slight to moderate discrimination between the adjacent soft tissues according to their physical density difference. On the CT images, bone appeared hyperdense, while tendons, ligament and hoof were appeared on various greyscale. Medulla of the bone had the dark shade (Figs 1–3). Proximal, middle and distal phalanx, proximal and distal sesamoid bones, superficial digital flexor tendon, deep digital flexor tendon and navicular bursa were clearly identified in CT images.

The skeleton of the metatarsus was formed in both animals, by the fused third and fourth metatarsal bones. In the camel, the fusion was incomplete where they still separated in the distal fifth (Figs 1–5).

The proximal extremity (base) of the fused third and fourth metatarsal bones showed internally a vertical bony septum (Fig. 1). The septum in the camel was extended

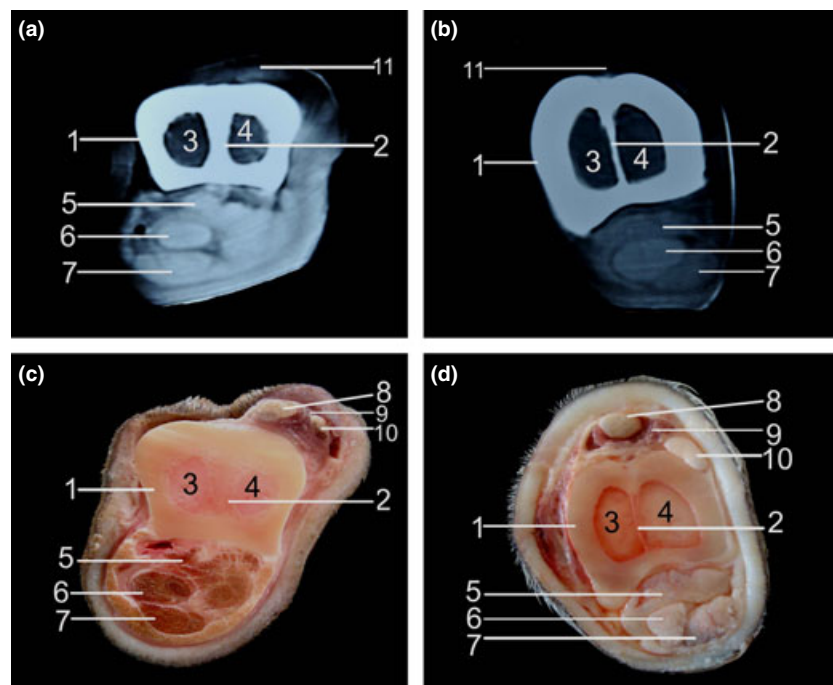


Fig. 1. Distal view of computed tomography and cross-section of the left metatarsus in the camel (a, c) and buffalo (b, d) at the level of the base of the large metatarsal bone, 3 cm distal to the carpal articular surface (dorsal is up and lateral is to the right of the viewer). 1 – Os metatarsale III et IV, 2 – Septum between fused third and fourth metatarsal bones, 3 – Cavum medullare ossis metatarsale III, 4 – Cavum medullare ossis metatarsale IV, 5 – M. inter-osseous, 6 – Tendo musculus flexor digitorum profundus, 7 – Tendo musculus flexor digitorum superficialis, 8 – Tendo musculus extensor digitorum longus, 9 – M. extensor digitorum brevis, 10 – Tendo musculus extensor digitorum lateralis, 11 – Extensor tendons (undifferentiated).

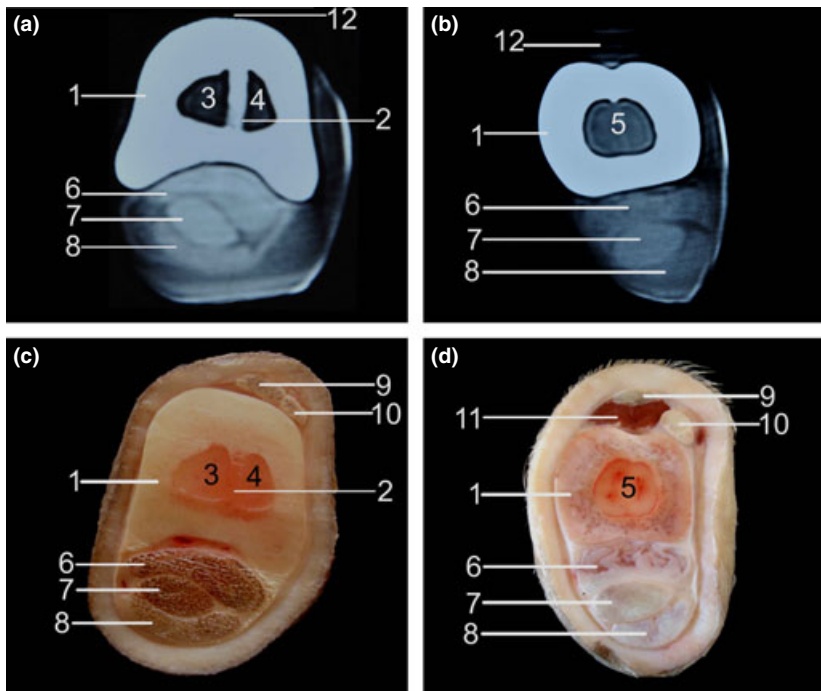


Fig. 2. Distal view of computed tomography and cross-section of the left metatarsus in the camel (a, c) and buffalo (b, d) at the level of the middle of the shaft of the large metatarsal bone. 1 – Os metatarsale III et IV, 2 – Septum between fused third and fourth metatarsal bones, 3 – Cavum medullare ossis metatarsale III, 4 – Cavum medullare ossis metatarsale IV, 5 – Cavum medullare ossis metatarsale III et IV, 6 – M. inter-osseus, 7 – Tendo musculus flexor digitorum profundus, 8 – Tendo musculus flexor digitorum superficialis, 9 – Tendo musculus extensor digitorum longus, 10 – Tendo musculus extensor digitorum lateralis, 11 – Tibialis cranialis muscle, 12 – Extensor tendons (undifferentiated).

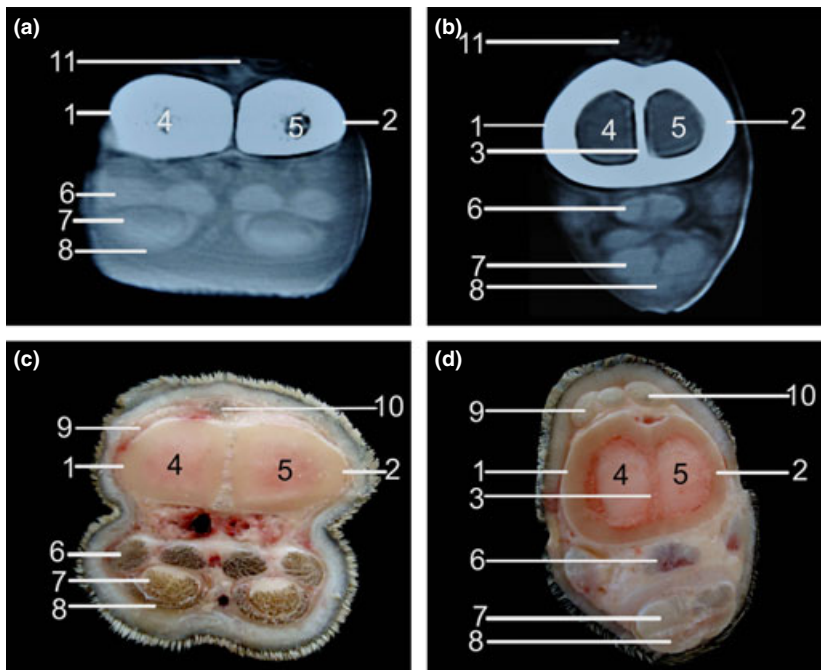


Fig. 3. Distal view of computed tomography and cross-section of the left metatarsus in the camel (a, c) and buffalo (b, d) at the level of the head (distal extremity) of the large metatarsal bone, 3 cm above the distal articular surface. 1 – Os metatarsale III, 2 – Os metatarsale IV, 3 – Septum between fused third and fourth metatarsal bones, 4 – Cavum medullare ossis metatarsale III, 5 – Cavum medullare ossis metatarsale IV, 6 – M. inter-osseus, 7 – Tendo musculus flexor digitorum profundus (divided), 8 – Tendo musculus flexor digitorum superficialis, 9 – Tendo musculus extensor digitorum longus, 10 – Tendo musculus extensor digitorum lateralis, 11 – Extensor tendons (undifferentiated).

along the line of the fusion of the two bones so it completely divided the medullary cavity. While in the buffalo, the septum was incomplete, extended for about 4–5 cm distal to the tarsal articular surface and partially divided the medullary cavity (Fig. 1).

The shaft of fused third and fourth metatarsal bones showed internally a vertical bony septum (Fig. 2). The

septum was complete in the camel and dividing the medullary cavity completely, but this septum was absent in the buffalo.

The distal extremity (head) of the fused third and fourth metatarsal bones in the buffalo showed internally a vertical bony septum (Fig. 3). The latter extended proximally for 4–5 cm, partially dividing the medullary cavity,

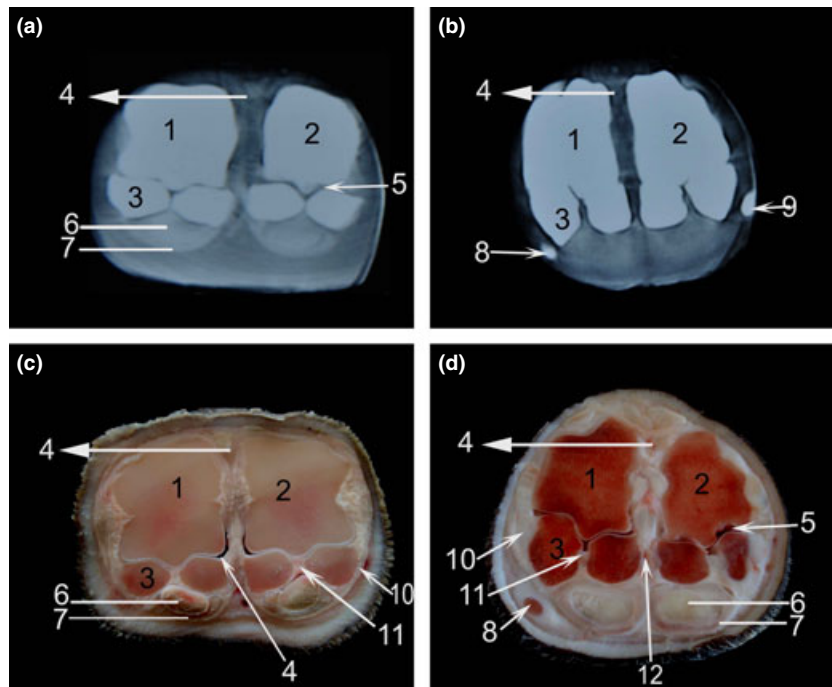


Fig. 4. Distal view of computed tomography and cross-section of the left metatarsus in the camel (a, c) and buffalo (b, d) at the level of the metatarsophalangeal (Fetlock). 1 – Caput ossis metatarsale III, 2 – Caput ossis metatarsale IV, 3 – Ossa sesamoidea proximalia, 4 – Incisura inter-trochlearis, 5 – Articulatio metatarsophalangea (Cavum articulare), 6 – Tendo musculus flexor digitorum profundus (divided), 7 – Tendo musculus flexor digitorum superficialis (Manica flexoria in buffalo), 8 – Digitus II, 9 – Digitus V, 10 – Ligg. Sesamoidea collateralia, 11 – Ligg. Plantaria, 12 – Lig. Inter-sesamoideum inter-digitale.

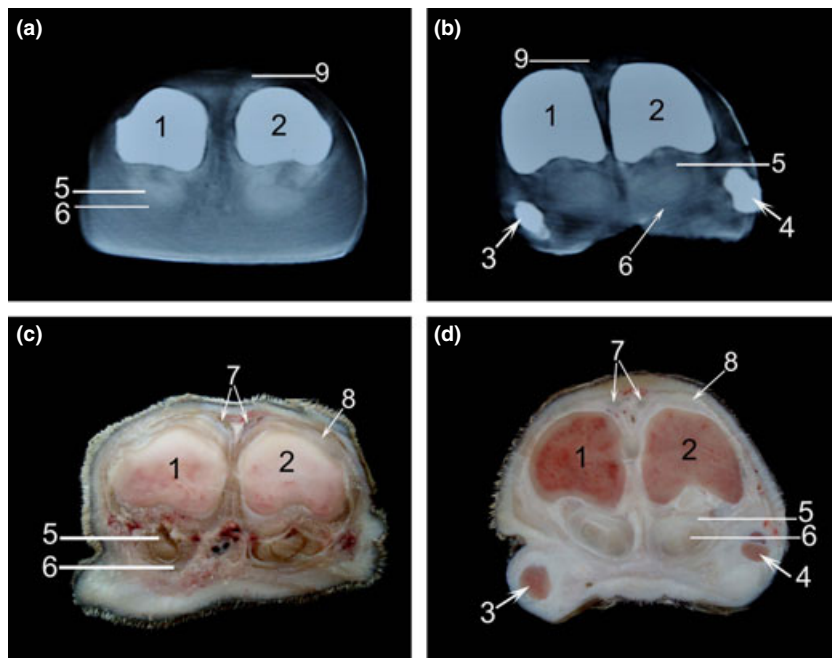


Fig. 5. Distal view of computed tomography and cross-section of the left hind digits in the camel (a, c) and buffalo (b, d) at the level of the base of the proximal phalanx. 1 – Basis phalangis proximalis digiti III, 2 – Basis phalangis proximalis digiti IV, 3 – Digitus II, 4 – Digitus V, 5 – Tendo musculus flexor digitorum superficialis (Manica flexoria in buffalo), 6 – Tendo musculus flexor digitorum profundus, 7 – Tendo musculus extensor digitorum longus, 8 – Tendo musculus extensor digitorum lateralis, 9 – Extensor tendons (undifferentiated).

while this septum was absent in the camel as the two metatarsi separated at the distal fifth.

In both animals, on the dorsal aspect of the fused third and fourth metatarsal bones, the tendon of *M. extensor digitorum longus* and the tendon of *M. extensor digitorum lateralis* (Figs 1–3) as well as *M. extensor digitorum brevis* (Fig. 1) were differentiated in the cross-sectional anatomy only when the intervening fascia dorsalis pedis

was dissected to demonstrate these tendons. These structures (extensor tendons) appeared in CT images as narrow transverse strap on the dorsal aspect of the fused third and fourth metatarsal bones, but the outline of each tendon was undifferentiated (Figs 1–3).

On the plantar aspect of the fused third and fourth metatarsal bones, in both species, the inter-osseous muscle (Figs 1–3) appeared more distinctly in the cross-sectional

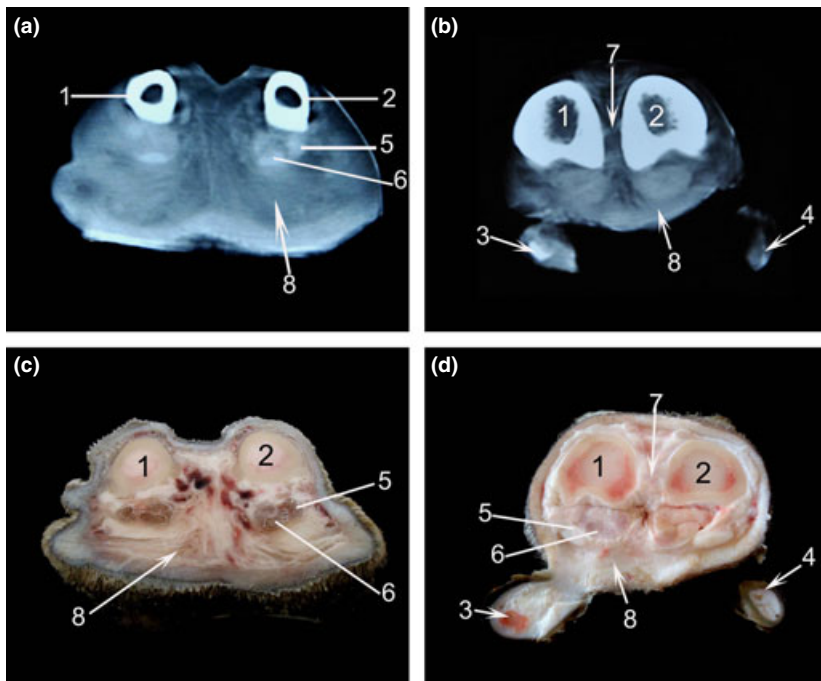


Fig. 6. Distal view of computed tomography and cross-section of the left hind digits in the camel (a, c) and buffalo (b, d) at the middle of the body (shaft) of the proximal phalanx. 1 – Corpus phalangis proximalis digiti III, 2 – Corpus phalangis proximalis digiti IV, 3 – Digitus II, 4 – Digitus IV, 5 – Tendo musculus flexor digitorum superficialis, 6 – Tendo musculus flexor digitorum profundus, 7 – Lig. Inter-digitale proximale, 8 – Tela subcutanea tori (Pulvinus digitalis or digital cushion).

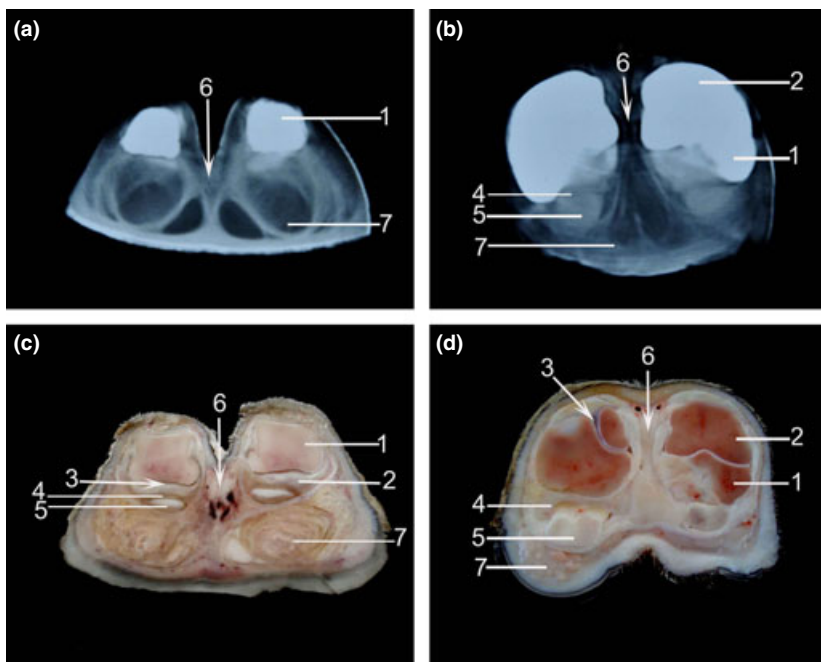


Fig. 7. Distal view of computed tomography and cross-section of the left hind digits in the camel (a, c) and buffalo (b, d) at the level of the proximal inter-phalangeal (pastern) joint. 1 – Basis phalangis mediae digiti IV, 2 – Caput phalangis proximalis digiti IV, 3 – Articulatio inter-phalangea proximalis pedis (Cavum articulare), 4 – Tendo musculus flexor digitorum superficialis, 5 – Tendo musculus flexor digitorum profundus, 6 – Lig. Inter-digitalia, 7 – Tela subcutanea tori (Pulvinus digitalis or digital cushion).

anatomy than in CT images. The deep digital flexor tendon and the superficial digital flexor tendon (Figs 1–3) were differentiated in the cross-sectional anatomy only when the intervening fascia plantaris was dissected to demonstrate these tendons. These structures (flexor tendons) appeared in CT images on the plantar aspect of the interosseous muscle and the fused third and fourth metatarsal bones; the outline of each tendon was differentiated.

The *Manica flexori* (Fig. 5) was a tubular sleeve (sheath) formed by the superficial digital flexor tendon and the inter-osseous muscle around the bifurcated deep digital flexor tendon in the vicinity of the metatarsophalangeal (fetlock) joint. It was clear in buffalo but not demonstrated in the camel.

At the level of metatarsophalangeal (fetlock) joints, in both animals, the axial and abaxial proximal sesamoid

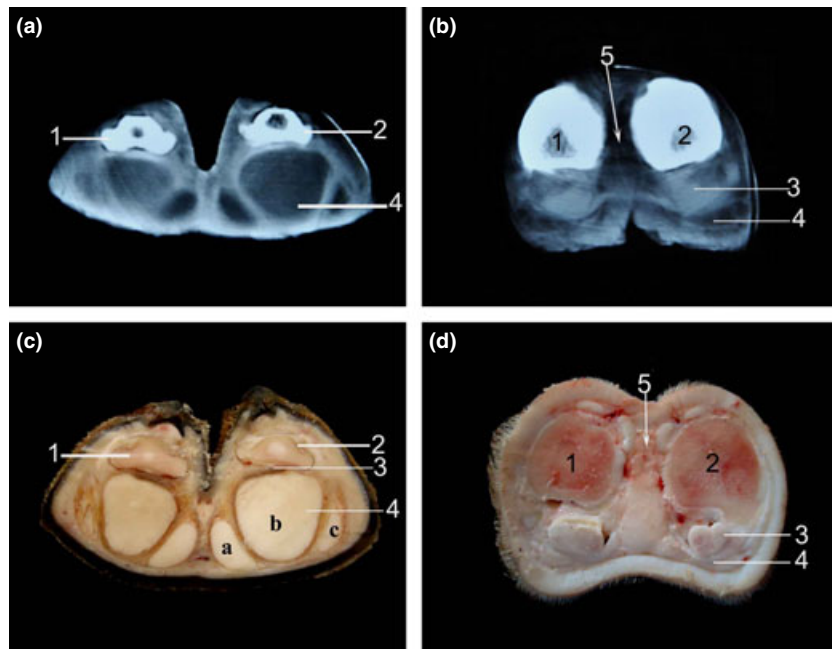


Fig. 8. Distal view of computed tomography and cross-section of the left hind digits in the camel (a, c) and buffalo (b, d) at the level of the body (shaft) of the middle phalanx. 1 – Corpus phalangis mediae digiti III, 2 – Corpus phalangis mediae digiti IV, 3 – Tendo musculus flexor digitorum profundus, 4 – Tela subcutanea tori (Pulvinus digitalis or digital cushion) (a – axial, b – middle and c – abaxial), 5 – Lig. Inter-digitalia distalis.

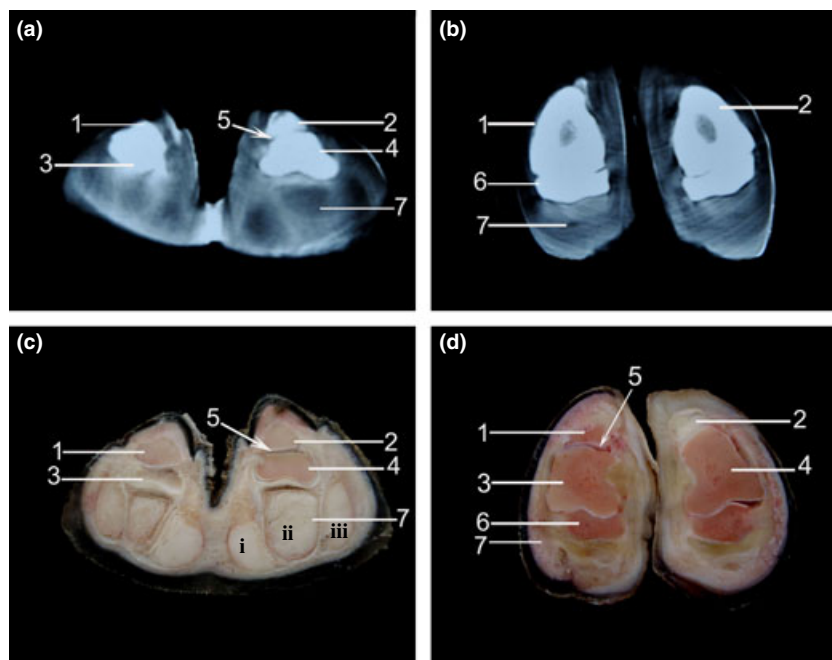


Fig. 9. Distal view of computed tomography and cross-section of the left hind digits in the camel (a, c) and buffalo (b, d) at the level of the distal inter-phalangeal (coffin) joint. 1 – Phalanx distale digiti III, 2 – Phalanx distale digiti IV, 3 – Caput phalangis mediae digiti III, 4 – Caput phalangis mediae digiti IV, 5 – Articulatio inter-phalangeae distalis pedis (Cavum articulare), 6 – Os sesamoideum distale, 7 – Tela subcutanea tori (Pulvinus digitalis or digital cushion) (i – axial, ii – middle and iii – abaxial).

bones were connected by a plantar ligament (Fig. 4). The two axial proximal sesamoid bones in the buffalo were connected together by the inter-digital inter-sesamoideum ligament (Fig. 4), the later was absent in the camel. Each abaxial proximal sesamoid bone was attached to the corresponding (medial or lateral) aspect of the head (distal extremity) of the fused third and fourth metatarsal bones by a collateral sesamoideum ligament (Fig. 4).

The second and fifth digits (Figs 4 and 5) of the buffalo appear in both CT and cross-section at the level of the base of the proximal phalanx, but these digits were absent in the camel.

In the camel, the inter-digital ligament (Fig. 7) connects the third and fourth digits at the level of the middle inter-phalangeal joint and continued to the level of the coffin joint. While in the buffalo, the proximal phalanges

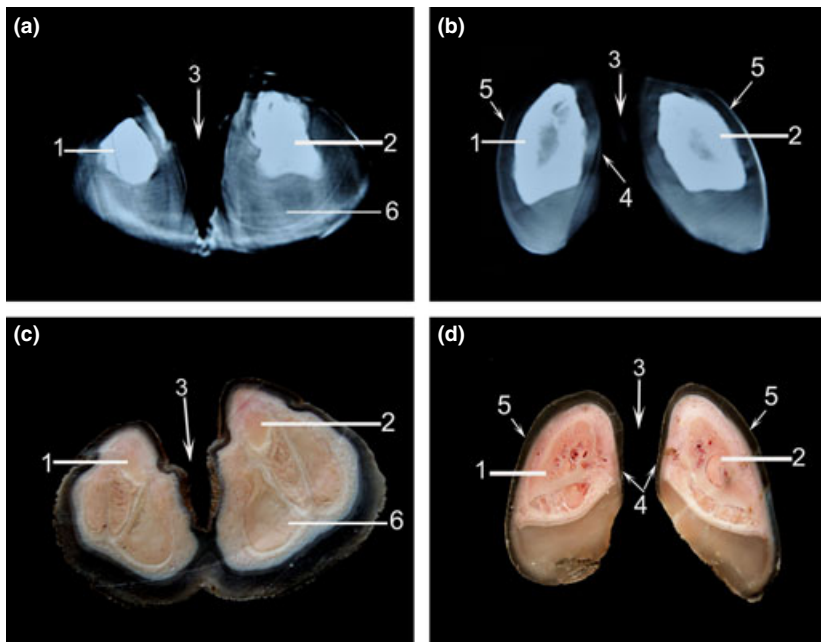


Fig. 10. Distal view of computed tomography and cross-section of the left hind digits in the camel (a, c) and buffalo (b, d) at a level of 1 cm below the distal inter-phalangeal (coffin) joint. 1 – Phalanx distale digiti III, 2 – Phalanx distale digiti IV, 3 – Spatium interdigitale, 4 – Pars axisialis paries corneus, 5 – Pars abaxialis paries corneus, 6 – Tela subcutanea tori (Pulvinus digitalis or digital cushion).

of the third and fourth digits were connected together along their inter-digital surfaces by the proximal inter-digital ligament (Fig. 6). The distal inter-digital ligament (Fig. 8) connected the third and fourth digits proximal to the inter-digital space.

At the level distal to the fetlock joint and prior to its insertion in the base of the middle phalanx, the flexor digitorum superficialis tendon gained a position deeper to that of the flexor digitorum profundus in both animals (Fig. 7).

The distal inter-phalangeal (coffin) joint (Fig. 9) is formed by articulation of the head of the middle phalanx, the distal phalanx and the distal sesamoid (navicular) cartilage in the camel and the distal sesamoid (navicular) bone in the buffalo (Fig. 9). The articular cavity (Fig. 9) was a potential cavity so it appeared linear in the cross-sectional anatomy, but did not appear in the CT images. The digital cushions in the camel were three: axial, middle and abaxial that appeared clearly in the CT images (Figs 8 and 9).

## Discussion

The present study served as an initial reference that aid in CT imaging diagnosis of the camel and buffalo metatarsus and digits disorders. Knowledge of normal cross-sectional anatomy of the camel and buffalo metatarsus and digits is essential for the evaluation of CT scans.

Computed tomography images of the camel and buffalo metatarsus and digits provide acceptable details of the anatomical structures and correlated well with corresponding gross specimens.

Computed tomography is able to discriminate physical density differences as small as 0.5%, whereas in conventional radiography, 10% physical density difference is needed for visual detection (Assheuer and Sager, 1997). Moreover, CT provides excellent spatial resolution and good discrimination between bone and soft tissues; this comes in agreement with that reported by previous studies (Peterson and Bowman, 1988; Feeney et al., 1991; Arencibia et al., 2000; Tomlinson et al., 2003 and Raji et al., 2008).

Computed tomography scan is an excellent imaging modality. Its usage in veterinary medicine is, however, limited as it is expensive and the animal should be anaesthetized (Arencibia et al., 2000). Nevertheless, it has some potential advantages over the routine radiography; it provides a cross-sectional image with superior soft tissue differentiation and no superimposition of the overlying structures, which can be used for better diagnosis of abnormalities (Raji et al., 2008).

The proximal and distal extremities of the fused third and fourth metatarsal bones in camels and buffaloes present a vertical bony septum internally that extend for 4–5 cm and partially dividing the medullary cavity in the buffalo. While in the camel, the vertical bone septum completely dividing the medullary cavity. So, this bone septum was devoid at the middle of the shaft of the fused third and fourth metatarsal bones in buffalo while it is complete in the camel which indicates that the metatarsus is reliable to the fracture in its middle part in the buffalo easier than in the camel.

The digital cushions were recognized in the CT images of camels, similar to that observed by Smuts and Bezuidenhout (1987) in the same species and by Weissengruber

et al. (2006) in the elephant. These cushions serve to absorb mechanical shock, store and return elastic strain energy, protect against local stress and keep pressures low (Ker, 1999 and Weissengruber et al., 2006). Neuville (1927) mentioned that the cushions of elephants exhibit similarities to the feet of humans, camels and rhinoceroses.

The adjacent extensor tendons appeared in CT images as transverse narrow strap, and the adjacent flexor tendons appeared in CT as roughly rounded mass, but the outline of each tendon was undifferentiated. This may be owing to a physical density difference <0.5% (Assheuer and Sager, 1997).

The undifferentiating of the outlines of the adjacent tendons in CT images is equivalent to cross-sectional anatomy without dissection of the intervening fascia, where the outlines did not appear in the latter also. Hence, cross-sectional anatomy is superior to CT only when the intervening fascia is dissected. Advantages, including depiction of detailed cross-sectional anatomy, improved contrast resolution and computer reformatting, make it a potentially valuable diagnostic technique. Thus, CT could be considered as a good tool for diagnosing diseases of the metatarsus and digits of the camel and buffalo.

The blood vessels that seen in cattle (Raji et al., 2008) could not be detected very well in the CT images in the present animals.

More benefits could be harvested from CT imaging when a future study is focused on certain part or joint or digits, especially when the inter-slicing space is decreased.

## Conclusion and Clinical Relevance

The knowledge of normal anatomy of the camel and buffalo metatarsus and digits on CT images is necessary to provide an accurate interpretation of these images. This study acts as a reference for the clinician who uses a CT for suspected abnormal limb.

## References

- Arencibia, A., J. M. Vazquez, M. Rivero, R. Latorre, J. A. Sandoval, J. M. Vilar, and J. A. Ramirez, 2000: Computed tomography of normal cranioccephalic structures in two horses. *Anat. Histol. Embryol.* **29**, 295–299.
- Assheuer, J., and M. Sager, 1997: MRI and CT Atlas of The Dog, 1st edn. Berlin, Wien, Oxford: Blackwell Science.
- Denoix, J. M., N. Crevier, B. Roger, and J. F. Lebas, 1993: Magnetic resonance imaging of the equine foot. *Vet. Radiol. Ultrasound* **6**, 405–411.
- Feeney, D., T. Fletcher, and R. Hardy, 1991: Atlas of Correlative Imaging Anatomy of the Normal Dog. Ultrasound and Computed Tomography. Philadelphia, PA: W B Saunders.
- Gehrmann, S., K. H. Höhne, W. Linhart, B. Pflesser, A. Pommert, M. Riemer, U. Tiede, J. Windolf, J. Schumacher, and M. Rueger, 2006: A novel interactive anatomic atlas of the hand. *Clin. Anat.* **19**, 258–266.
- Getty, R., 1975: The Anatomy of the Domestic Animals, 5th edn, Vol. 1. Philadelphia, London, Toronto: WB Saunders Co., pp. 993–1002, 1141–1147.
- Kaser-Hotz, B., S. Sartoretti-Schefer, and R. Weiss, 1994: Computed tomography and magnetic resonance imaging of the normal equine carpus. *Vet. Radiol. Ultrasound* **6**, 457–461.
- Ker, R. F., 1999: The design of soft collagenous load-bearing tissues. *J. Exp. Biol.* **202**, 3315–3324.
- Neuville, H., 1927: Note préliminaire sur l'organisation du pied des éléphants. *Bull. Mus. Natl d'Histoire Naturelle* **33**, 60–64.
- Nickel, R., A. Schummer, and E. Seiferle, 1996: The Anatomy of Domestic Animals, Vol. 2. Oxford: Blackwell Science, pp. 69–71, 428–432, 191–197.
- Nomina Anatomica Veterinaria, 2005: International Committee on Veterinary Gross Anatomical Nomenclature of the World Association of Veterinary Anatomists, 5th edn. Hannover, Columbia: Gent, Sapporo.
- Ottesen, N., and L. Moe, 1998: An introduction to computed tomography (CT) in the dog. *Eur. J. Companion Anim. Pract.* **8**, 29–36.
- Peterson, P. R., and K. F. Bowman, 1988: Computed tomographic anatomy of the distal extremity of the horse. *Vet. Radiol. Ultrasound* **29**, 147–156.
- Raji, A. R., K. Sardari, and H. R. Mohammadi, 2008: Normal cross-sectional anatomy of the bovine digit: comparison of computed tomography and limb anatomy. *Anat. Histol. Embryol.* **37**, 188–191.
- Schaller, O., 1992: Illustrated Veterinary Anatomical Nomenclature. Stuttgart: Enke Verlag.
- Shearer, J. K., and S. R. Van Amstel, 2001: Functional and corrective claw trimming. *Vet. Clin. North Am. Food Anim. Pract.* **171**, 53–72.
- Smuts, M. S., and A. J. Bezuidenhout, 1987: Anatomy of the Dromedary. Oxford: Clarendon Press.
- Tomlinson, J. E., W. R. Redding, C. Berry, and J. E. Smallwood, 2003: Computed tomographic anatomy of the equine tarsus. *Vet. Radiol. Ultrasound* **44**, 174–178.
- Weissengruber, G. E., G. F. Egger, J. R. Hutchinson, H. B. Groenewald, L. Elsässer, D. Famini, and G. Forstenpointner, 2006: The structure of the cushions in the feet of African elephants (*Loxodonta African*). *J. Anat.* **209**, 781–792.
- Whitton, R. C., C. Buckley, T. Donovan, A. D. Wales, and R. Dennis, 1998: The diagnosis of lameness associated with distal limb pathology in a horse: a comparison of radiography, computed tomography and magnetic resonance imaging. *Vet. J.* **155**, 223–229.